HHS Public Access

Author manuscript

Eur J Nucl Med Mol Imaging. Author manuscript; available in PMC 2015 May 01.

Published in final edited form as:

Eur J Nucl Med Mol Imaging. 2009 August ; 36(8): 1273–1282. doi:10.1007/s00259-009-1089-x.

PET imaging of HSV1-tk mutants with acquired specificity toward pyrimidine- and acycloguanosine-based radiotracers

Yury Likar,
Molecular Imaging Laboratory, Department of Radiology, Memorial Sloan-Kettering Cancer Center, 1275 York Ave, (Box 501) Z-2035, New York, NY 10021, USA

Konstantin Dobrenkov,
Molecular Imaging Laboratory, Department of Radiology, Memorial Sloan-Kettering Cancer Center, 1275 York Ave, (Box 501) Z-2035, New York, NY 10021, USA

Malgorzata Olszewska,
Molecular Imaging Laboratory, Department of Radiology, Memorial Sloan-Kettering Cancer Center, 1275 York Ave, (Box 501) Z-2035, New York, NY 10021, USA

Larissa Shenker,
Molecular Imaging Laboratory, Department of Radiology, Memorial Sloan-Kettering Cancer Center, 1275 York Ave, (Box 501) Z-2035, New York, NY 10021, USA

Shangde Cai,
Radiochemistry/Cyclotron Core Facility, Memorial Sloan-Kettering Cancer Center, New York, NY 10021, USA

Hedvig Hricak, and
Molecular Imaging Laboratory, Department of Radiology, Memorial Sloan-Kettering Cancer Center, 1275 York Ave, (Box 501) Z-2035, New York, NY 10021, USA

Vladimir Ponomarev
Molecular Imaging Laboratory, Department of Radiology, Memorial Sloan-Kettering Cancer Center, 1275 York Ave, (Box 501) Z-2035, New York, NY 10021, USA

Yury Likar: likary@mskcc.org; Vladimir Ponomarev: ponomarv@mskcc.org

Abstract

Purpose—The aim of this study was to create an alternative mutant of the herpes simplex virus type 1 thymidine kinase (HSV1-tk) reporter gene with reduced phosphorylation capacity for acycloguanosine derivatives, but not pyrimidine-based compounds that will allow for successful PET imaging.

Methods—A new mutant of HSV1-tk reporter gene, suitable for PET imaging using pyrimidine-based radiotracers, was developed. The HSV1-tk mutant contains an arginine-to-glutamine substitution at position 176 (HSV1-R176Qtk) of the nucleoside binding region of the enzyme.

Correspondence to: Vladimir Ponomarev, ponomarv@mskcc.org.

Results—The mutant-gene product showed favorable enzymatic characteristics toward pyrimidine-based nucleosides, while exhibiting reduced activity with acycloguanosine derivatives. In order to enhance HSV1-R176Qtk reporter activity with pyrimidine-based radiotracers, we introduced the R176Q substitution into the more active HSV1-sr39tk mutant. U87 human glioma cells transduced with the HSV1-R176Qsr39tk double mutant reporter gene showed high ^{3}H-FEAU pyrimidine nucleoside and low ^{3}H-penciclovir acycloguanosine analog uptake in vitro. PET imaging also demonstrated high ^{18}F-FEAU and low ^{18}F-FHBG accumulation in HSV1-R176Qsr39tk+ xenografts. The feasibility of imaging two independent nucleoside-specific HSV1-tk mutants in the same animal with PET was demonstrated. Two opposite xenografts expressing the HSV1-R176Qsr39tk reporter gene and the previously described acycloguanosine-specific mutant of HSV1-tk, HSV1-A167Ysr39tk reporter gene, were imaged using a short-lived pyrimidine-based ^{18}F-FEAU and an acycloguanosine-based ^{18}F-FHBG radiotracer, respectively, administered on 2 consecutive days.

Conclusion—We conclude that in combination with acycloguanosine-specific HSV1-A167Ysr39tk reporter gene, a HSV1-tk mutant containing the R176Q substitution could be used for PET imaging of two different cell populations or concurrent molecular biological processes in the same living subject.

Keywords

Molecular imaging; Reporter gene; HSV1-tk; PET; FEAU; FHBG

Introduction

During the past decade, a number of reports showed the advantage of using herpes simplex virus type 1 thymidine kinase (HSV1-tk) as a suicide gene in combination with ganciclovir (GCV) [1] and a nuclear imaging reporter gene when used with an appropriate reporter probe [2–5]. Unlike other reporter proteins, HSV1-tk phosphorylates a wide range of substrates: pyrimidine (uracil-based FIAU, FEAU, FFEAU) and purine [acycloguanosine-based penciclovir (PCV), FHBG, FHPG)] nucleoside analogs labeled with short- (^{11}C, ^{18}F) and long-lived (^{123}I, ^{124}I, ^{125}I, ^{131}I) radioisotopes [2, 6–9]. Specific accumulation of a number of these substrates has been demonstrated in wild-type HSV1-tk or mutant HSV1-sr39tk expressing cells in vitro and in vivo. It has been shown that wild-type HSV1-tk has preferential activity toward pyrimidine-based compounds, while mutant HSV1-sr39tk can efficiently phosphorylate both types of derivatives [10–13].

Positron emission tomography (PET) has been used in experimental models and clinical trials to evaluate responses to HSV1-tk-mediated suicide gene therapy [14– 17], to track the migration of HSV1-tk-expressing cells [18–20], and non-invasively assess the activity of endogenous gene expression [21–23]. In the situations, where one needs to image the location, viability, and proliferation of two different cell populations in the same animal (for example, both a tumor cell population and antitumor lymphocytes that migrate to the tumor), each cell population must express a different PET reporter gene that can be imaged separately with two different shortlived radiotracers. In this context, the development of new mutant of HSV1-tks with restricted specificity toward pyrimidine- or acycloguanosine-based radiotracers would be very useful.

Lately, our group has described a new human-derived reporter gene, namely, human delta mitochondrial thymidine kinase type 2 (hΔTK2), which is intrinsically restricted to pyrimidine-based nucleoside derivatives [24]. We have shown that cells transduced with this reporter gene do not accumulate acycloguanosine derivatives and can be imaged with pyrimidine-based radiotracers. However, cells expressing hΔTK2 show relatively low levels of accumulation of pyrimidine derivatives when directly compared with HSV1-tk (six- to tenfold). Therefore, we aimed to work on HSV1-tk as a more promising contender.

We have recently reported on a new mutant of HSV1-tk, HSV1-A167Ysr39tk, which combines an acycloguanosine-restricting alanine-to-tyrosine substitution at position 167 and five amino acid substitutions (positions 159–161, 168, 169) from the HSV1-sr39tk mutant (Fig. 1) [25]. This mutant lacks the ability to phosphorylate pyrimidine-based nucleoside derivatives, including antiviral drugs (BVdU, brivudine, Zostex, Berlin-Chemie, Berlin, Germany) and several uracil-based radiotracers (FIAU, FEAU). However, the HSV1-A167Ysr39tk mutant gene product retains high phosphorylation activity with acycloguanosine analogs, including ^{18}F-FHBG for PET imaging and GCV for suicide safety concerns.

The aim of this study was to create an alternative mutant of the HSV1-tk reporter gene with reduced phosphorylation capacity for acycloguanosine derivatives, but not pyrimidine-based compounds that will allow for successful PET imaging. We approached this problem by reviewing HSV1-tk mutants derived from drug-resistant strains of the virus with reduced activity toward pyrimidine and/or acycloguanosine substrates [26]. One, an acyclovirresistant mutant bearing arginine-to-glutamine substitution at position 176 (R176Q), showed favorable enzymatic characteristics toward pyrimidine-based nucleosides, while exhibiting near complete absence of activity with acycloguanosine derivatives. We hypothesized that in combination with acycloguanosine-specific HSV1-A167Ysr39tk reporter gene, a HSV1-tk mutant containing the R176Q mutation could be potentially used for PET imaging of two independent cell populations or molecular biological processes in the same living subject using consecutive administration of short-lived pyrimidine- (^{18}F-FIAU, ^{18}F-FEAU) and acycloguanosine- (^{18}F-FHBG) based radiotracers.

Materials and methods

Retroviral vectors

The schematic structures of the retroviral vectors used in this study are shown in Fig. 1. A retroviral vector containing a wild-type HSV1-tk reporter gene with a nuclear export signal (NES) from MAPKK of *Xenopus*, SFG-Nes-wild type-HSV1-tk/GFP (wild-type HSV1-tk), was described previously [27] and served as a reference vector. The HSV1-sr39tk mutant (kindly provided by SS Gambhir, Stanford, CA, USA, Fig. 1a), was introduced into SFG-Nes-wild-type HSV1-tk/GFP vector replacing the wild-type HSV1-tk, which resulted in SFG-Nes-HSV1-sr39tk/GFP (HSV1-sr39tk) retroviral vector. An arginine-to-glutamine substitution at position 176 in the wild-type HSV1-tk and HSV1-sr39tk genes was performed using the following primer pairs: 5′-TACCCGGCCGCGCAATACCTTATGGGC-3′ and 5′-GCCCATAAGGTATTGCGCGGCCGGGTA-3′ for SFG-Nes-HSV-tk/GFP and for SFG-

NesHSV1sr39tk/GFP vectors, resulting in SFG-Nes-HSV1-R176Qtk/GFP (HSV1-R176Qtk) and SFG-Nes-HSV1-R176Qsr39tk/GFP (HSV1-R176Qsr39tk) retroviral vectors, respectively.

Transduction of tumor cells

The U87 human glioma cell line (ATCC, Rockville, MD, USA) was grown as monolayers in MEM media at 37°C. The in vitro transduction of U87 cells with the retroviral vectors was accomplished by exposing the cell monolayers to a filtered (0.45 μm) culture medium obtained from the vector producer H29GPG cells [28] for 8 h in the presence of polybrene (8 μg/ml, Sigma, St. Louis, MO, USA).

Flow cytometry and fluorescent microscopy

Retrovirally transduced U87 cells were grown as bulk cultures for 48 h and subsequently sorted for GFP expression using FACS (FACSVantage, Becton Dickinson, St. Jose, CA, USA); the 488-nm excitation beam and 510-nm emission filters were used. Subcellular localization of the reporter proteins in transduced tumor cells was visualized by fluorescence microscopy (Nikon, Osaka, Japan) using similar excitation and emission parameters.

Quantitative reverse transcription polymerase chain reaction (RT-PCR)

Total RNA was isolated from cells that were previously transfected with the HSV1-tk/GFP fusion gene and its mutants as described above. For quantitative RT-PCR, reverse transcription was carried out using the First-Strand cDNA Synthesis kit (Amersham Biosciences, Fairfield, CT, USA) with NotId(T)18 primers. The quantitative PCR was performed using the QuantiTect SYBR green PCR kit (Qiagen, Valencia, CA, USA) and analyzed on an Light-Cycler system (Roche Diagnostics, Indianapolis, IN, USA) using the LightCycler software version 3 (Roche Diagnostics, Indianapolis, IN, USA). Quantitative PCRs were carried out to detect HSV1-tk/GFP mRNA and its mutants using the following primer sets: (5′-AGCAAGAAGCCACGGAAGT-3′ and 5′-TCCCGTGAGGACCGTCTAT-3′). The data were normalized to the amount of β-actin RNA in each sample using a commercial kit (Stratagene, La Jolla, CA, USA) and then compared to a standard curve HSV1-tk/GFP plasmid to determine the amount of each mRNA in the starting sample. RNAs isolated were each assayed in duplicate and the data were averaged.

Western blot analysis

Cells were lysed in M-PER mammalian protein extraction reagent (Pierce Biotechnology, Rockford, IL, USA) for 10 min at 4°C. After lysis, cell debris were removed by microcentrifugation (14,000 *g* for 15 min at 4°C), and the total cell protein concentration for each sample was determined using a BCA protein assay kit (Thermo Fisher Scientific, Fremont, CA, USA) according to the manufacturer's instructions. Equal amounts of sample protein were combined with Full Range Rainbow recombinant protein molecular weight marker (GE Healthcare, Waukesha, WI, USA) and heated for 10 min at 95°C. Extracted proteins were run on NuPage 4-12% Bis-Tris polyacrylamide gel (Invitrogen, Carlsbad, CA, USA). The separated proteins were transferred to Invitrolon™ PVDF membranes

(Invitrogen, Carlsbad, CA, USA) using an XCell SureLock™ blotting system and NuPage® buffer (Invitrogen, Carlsbad, CA, USA). Membranes were incubated in 15% hydrogen peroxide for 10 min and blocking buffer (Tris-buffered saline with 1.0% non-fat dried milk, 0.4% fish tail gelatin, and 0.1% bovine serum albumin) for 2 h. All subsequent incubations and washes were in TBS/T (Tris-buffered saline with 0.1% Triton X-100). Primary and secondary antibody incubations (1:3,000 dilutions for each) were for 40 min each, followed by 20 washes of 50 ml TBS/T for 2 min each. Proteins were detected using mouse monoclonal antibody-specific for GFP (clone 7.1, Roche Diagnostics, Indianapolis, IN, USA) and mouse β-actin-specific antibodies (Bio-Rad, Hercules, CA, USA), alkaline phosphatase (AP)-conjugated goat anti-mouse antibody (Bio-Rad, Hercules, CA, USA) and AP-specific color development solution (Bio-Rad, Hercules, CA, USA) for visualization. Chemiluminescence signals were collected on the Epi ChemiDoc imager (Bio-Rad, Hercules, CA, USA) and quantified with QuantiOne Analysis Software (Bio-Rad, Hercules, CA, USA).

FEAU and PCV in vitro accumulation assay

The ^{3}H-FEAU and ^{3}H-PCV accumulation assays were performed as previously described [2]. Briefly, cells were seeded in 150×25-mm tissue culture plates (Nunc, Roskilde, Denmark) at a concentration of 2×10^{6} cells/plate and grown until 50–60% confluence. The incubation medium contained ^{3}H-FEAU 3.7 kBq/ml (1.48 TBq/mmol) or ^{3}H-PCV 3.7 kBq/ml (1.11 TBq/mmol) (Moravek Biochemicals, Brea, CA, USA, purity >99%). The cells were harvested after various periods of incubation (30, 60, and 120 min), centrifuged, cell pellets were weighed, and assayed for radioactivity concentration using a TriCarb 1600 beta spectrometer (Packard, Downers Grove, IL, USA) using the standard ^{3}H channel counting technique. The data were expressed as a harvested cell to medium concentration ratio: (dpm/g cells)/(dpm/ml medium). The rates of accumulation (Ki) for FEAU and PCV were determined from the slope of the cell to medium ratios versus incubation time plots and have units of tracer clearance from the medium (ml medium/min/g cells).

Prodrug sensitivity assays

To determine the cytotoxic effect (IC_{50}) of GCV (CYTOVENE-IV; Roche Laboratories Inc., Nutley, NJ, USA) and BVdU ((E)-5-(2-bromovinyl)-2′-deoxyuridine, Sigma-Aldrich, St. Louis, MO, USA) on non-transduced and transduced U87 cells, a WST-1 (Roche, Mannheim, Germany) cell viability assay was performed 4 days after exposure to the drugs. Cells were plated into 96-well microtiter plates at an initial density of 4,000 cells/well; GCV or BVdU were added to sets of eight wells for each concentration tested. The drug concentrations ranged from 1 nM to 10 mM.

Experimental groups of animals

All animal studies were performed under a Memorial Sloan-Kettering Cancer Center IACUC-approved protocol. Six- to eight-week-old nude mice from Taconic (Germantown, NY, USA) were used; 5×10^{6} cells for each tumor were implanted. Four groups of animals (n=10/group) were studied, and three xenografts were produced in each animal. U87/non-transduced (N/T) and U87/HSV1-R176Qsr39tk xenografts were established in the left thigh

and right shoulder, respectively, of each animal in all groups. The third xenograft was established in the left shoulder from U87/wild-type HSV1-tk, U87/HSV1-R176Qtk, U87/HSV1-sr39tk, and U87/HSV1-A167Ysr39tk cells in groups 1, 2, 3, and 4, respectively. The mice were anesthetized using 2:98% isoflurane:oxygen gas mixture. All animals were sacrificed using CO_2 inhalation.

PET imaging with ^{18}F-FEAU and ^{18}F-FHBG

The animals were monitored daily for tumor growth. Imaging studies were performed when subcutaneous tumors reached ~10 mm in diameter. ^{18}F-FEAU [29] and ^{18}F-FHBG were prepared as previously described [30]. MicroPET imaging was performed 2 h after i.v. administration of 7.4 MBq (200 μCi) of ^{18}F-FEAU (specific activity 37 TBq/mmol) to each animal. After the ^{18}F-radioactivity decay (24 h later), the same animals were injected i.v. with 7.4 MBq (200 μCi) of ^{18}F-FHBG (specific activity 44.4 TBq/mmol) and imaged 2 h later. PET imaging was performed using a FOCUS 120 microPET™ scanner (Siemens Preclinical Solutions, Knoxville, TN, USA). At least 10 million coincidence events were acquired per study using a 350–750 keV energy window and a 6-ns timing window. List-mode data were sorted into sinograms by Fourier rebinning and reconstructed by filter back-projection without attenuation or scatter correction. Count data in the reconstructed images were converted to activity concentration [i.e., % of the injected dose per cc (%ID/cc)] based on a system calibration factor determined using a ^{18}F-filled mouse-size phantom. Visualization and analyses of microPET images were carried out using AsiPRO™ software (Siemens Preclinical Solutions, Knoxville, TN, USA). Radioactivity concentration in tissue was calculated from the microPET images using maximum pixel values. Reporter gene selectivity index in vivo was calculated as a ratio between ^{18}F-FEAU and ^{18}F-FHBG activity concentrations in the same tumor.

Tissue sampling and radioactivity measurements

Immediately after the ^{18}F-FEAU and ^{18}F-FHBG imaging sessions five animals from each group were sacrificed. Tumors and muscle tissue were excised, washed, and weighted. The radioactivity concentration in tissue samples was measured using a gamma counter (Model A5550, Packard, United Technologies, Hartford, CT, USA), normalized to sample weight and expressed as the percentage of injected dose per gram of tissue (%ID/g).

Statistical analysis

All data obtained in in vitro and in vivo studies were compared using Student's *t* test for independent samples with unequal variances. Mean values and independent *t* test for unequal variances were calculated using Graph Prism 4 software (GraphPad Software, San Diego, CA, USA). Values of $p<0.05$ were considered statistically significant.

Results

Characterization of reporter genes in vitro

GFP-positive populations with similar levels of GFP expression (~500 fluorescent units) were obtained. Following FACS sorting, all cell lines were >96% GFP+ (Fig. 1a-e). Fluorescent microscopic analysis demonstrated cytoplasmic distribution of Nes-wild-type

HSV1-tkGFP, Nes-HSV1-R176QtkGFP, Nes-HSV1-sr39tkGFP, and Nes-HSV1-R176Qsr39tk reporter proteins due to the presence of NES signal at the N terminus (data not shown).

When normalized to (β-actin housekeeping gene expression, RT-PCR analysis showed similar levels of HSV1-tk/GFP mRNA expression from different transduced cell populations (Fig. 1f). The HSV1-tk/GFP and (β-actin proteins had the predicted molecular mass of ∼72 (full length HSV1-tk/GFP) and ∼42 kDa, respectively, and were uniformly expressed in all transduced cells as determined by Western blot analysis (Fig. 1g).

The levels of enzymatic activity of wild-type HSV1-tk, HSV1-R176Qtk, HSV1-sr39tk, and HSV-R176Qsr39tk proteins were assessed using a previously established radiotracer accumulation assay with ^{3}H-FEAU and ^{3}H-PCV (Fig. 2). Since the level of reporter expression was similar in all transduced cell lines, the radiotracer accumulation (Ki) values can be directly compared. In non-transduced U87 cells background levels of ^{3}H-FEAU and ^{3}H-PCV uptake were detected. ^{3}H-FEAU was accumulated in all transduced cells except HSV-A167Ysr39tk compared to non-transduced U87 cells. Wild-type HSV1-tk, HSV1-sr39tk, and HSV-R176Qsr39tk cells showed high levels of ^{3}H-FEAU uptake (Ki of 0.43, 0.73, and 0.33 ml/min per g cells, respectively), while HSV1-R176Qtk cells showed significantly ($p<0.01$) lower ^{3}H-FEAU uptake (Ki of 0.035). ^{3}H-PCV accumulation was significantly ($p<0.05$) lower in HSV1-R176Qtk, HSV-R176Qsr39tk, and wildtype HSV1-tk (Ki of 0.018, 0.019, and 0.035 ml/min per g cells, respectively) compared with HSV1-sr39tk and HSV-A167Ysr39tk transduced cells (Ki of 0.79 and 0.4 ml/min per g cells, respectively).

To explore the possibility of killing transduced cells using a “suicide” prodrug activation strategy, the sensitivity of wild-type and transduced U87 cells to GCV and BVdU was assessed (Fig. 3). HSV1-R176Qtk- and HSV1-R176Qsr39tk-expressing cells were equally sensitive to BVdU (IC_{50} of 92 and 91 μM, respectively), but showed different IC_{50} values with GCV (940 and 111 μM, respectively). Wild-type U87 cells were highly resistant to BVdU and GCV (IC_{50} >10 and >1 mM, respectively)

In vivo imaging of reporter gene expression with PET

The initial microPET imaging studies were performed in the first three groups of mice bearing s.c. xenografts derived from wild-type HSV1-tk, HSV1-sr39tk, HSV1-R176Qtk, and HSV-R176Qsr39tk transduced U87 cell populations and wild-type U87 cells which served as a negative control (Fig. 4a,b). Since the level of reporter expression was similar in the cell lines used to produce the xenografts (Fig. 1), the images and the level of radioactivity can be directly compared. The levels of ^{18}F-FEAU and ^{18}F-FHBG radioactivity in control (non-transduced) U87 tumors were very low and similar to body background. MicroPET imaging revealed high localization of ^{18}F-FEAU-derived radioactivity in xenografts expressing wildtype HSV1-tk, HSV1-sr39tk, and HSV1-R176Qsr39tk reporter genes (Fig. 4a,b). ^{18}F-FEAU accumulation was low in xenografts derived from HSV1-R176Qtk transduced cells, but significantly higher ($p<0.01$) when compared with N/T cells. As shown in the in vitro studies, ^{18}F-FHBG accumulation was high in HSV1-sr39tk xenografts and wild-type HSV1-tk, however significantly reduced in

HSV1-R176Qtk+ and HSV1-R176Qsr39tk+ xenografts. U87/wild-type HSV1-tk had significantly higher ^{18}F-FHBG uptake compared to HSV1-R176Qtk+ and HSV1-R176Qsr39tk xenografts (four and twofold, respectively, $p<0.05$) (Fig. 4a,b). Tissue sampling and biodistribution studies confirmed highly specific ^{18}F-FEAU accumulation in U87/wild-type HSV1-tk, U87/HSV1-sr39tk, and U87/HSV1-R176Qsr39tk tumors (Fig. 4c). The non-transduced U87 tumors and muscle tissue showed only low background levels of radioactivity. Selectivity indexes (ratios between ^{18}F-FEAU and ^{18}F-FHBG activity concentrations in the same tumors) in vivo for wild-type HSV1-tk, HSV1-sr39tk, HSV1-R176Qtk, and HSV1-R176Qsr39tk reporter genes were 4.3, 0.9, 2.2, and 6.0, respectively.

In a separate (fourth) group of mice, specific ^{18}F-FEAU accumulation was observed in U87/HSV1-R176Qsr39tk tumors, while HSV-A167Ysr39tk-expressing xenografts did not show any evidence of ^{18}F-FEAU uptake. In contrast, ^{18}F-FHBG accumulation was high in U87/HSV-A167Ysr39tk+ tumors with only slight uptake in U87/HSV1-R176Qsr39tk+ xenografts (Fig. 5).

Discussion

The enzyme, wild-type HSV1 thymidine kinase (HSV1-tk), can phosphorylate pyrimidine and purine nucleotides derivatives. Radiolabeled pyrimidine-based (^{124}I-FIAU, ^{18}F-FIAU, ^{18}F-FEAU, ^{18}F-FFEAU, and ^{18}F-FMAU [3, 31–35]) and acycloguanosine-based (^{18}F-GCV, ^{18}F-FHBG, and ^{18}F-FHPG [4, 36–38]) nucleoside analogs have been used to image HSV1-tk and HSV1-sr39tk reporter gene expression with PET. However, the ability of HSV1-tk and HSV1-sr39tk reporter proteins to phosphorylate both pyrimidine and acycloguanosine analogs does not allow imaging with different groups of radiolabel consecutively and we can evaluate only single events. Since the availability of two in vivo reporter genes will be of considerable utility for simultaneous imaging of two independent cell populations or molecular biological processes, we aimed at developing and testing new mutants of the HSV1-tk reporter gene family that would exhibit selective specificity toward pyrimidine- or acycloguanosine-based radiotracers.

We focused on modifications of HSV1-tk reporter gene for several reasons. First, HSV1-tk is a well-known reporter gene and has demonstrated safety and efficacy in experimental and clinical studies. Second, HSV1-tk can be used as a “safety switch” due to its ability to phosphorylate clinically used nucleoside suicide prodrugs. Unlike many other reporter gene—reporter probe combinations, expression of HSV1-tk can be imaged using both long-lived ^{124}I and, most importantly, short-lived ^{18}F and ^{11}C radioisotopes [6]. The latter feature allows consecutive imaging of the HSV1-tk mutants we have developed with clinically applicable pyrimidine- and acycloguanosine-based radiotracers on a daily basis (^{18}F) or even during the same day (^{11}C).

Several groups have performed genetic modifications of the wild-type HSV1-tk that resulted in mutants with enhanced phosphorylation kinetics for certain nucleoside derivatives [39, 40]. The widely used HSV1-sr39tk mutant, bearing five amino acid substitutions in the nucleoside binding region of the enzyme [13, 41] (Fig. 1), shows significantly improved activity with acycloguanosines, specifically GCV, ACV, PCV, and ^{18}F-FHBG, but preserve

the activity with pyrimidine analogs [11]. In a recent study we have shown that position 167 [25] in HSV1-tk protein is particularly favorable for discriminating between pyrimidine and acycloguanosine substrates. A HSV1-sr39tk mutant bearing the alanine-167-tyrosine (A167Y) substitution in nucleoside binding region, HSV1-A167Ysr39tk reporter, showed a markedly decreased activity with the clinically relevant pyrimidines (ARA-T and BVdU in particular) and pyrimidine-based radiotracers (^{18}F-FIAU and ^{18}F-FEAU), while phosphorylation of GCV, PCV, and ^{18}F-FHBG was preserved.

While searching for a pyrimidine-specific variant of HSV1-tk, several antiviral drug-resistant isolates of HSV1 have been found [26]. Several strains carrying a mutation in the thymidine kinase gene show partial or complete lack of phosphorylation of clinically used pyrimidine and acycloguanosine derivatives. We studied a mutant bearing an arginine-to-glutamine substitution at position 176, because of its favorable enzymatic characteristics toward pyrimidine-based nucleosides. It has been shown that this mutation seems to have only local effects on the substrate-binding site, whereas the folding of the protein remains the same. First, we evaluated HSV1-R176Qtk fused with GFP in U87 human glioma cells. We found that cells expressing this mutant did not show any accumulation of ^{3}H-PCV, while ^{3}H-FEAU uptake was low, but above background levels. These results suggested that further mutation of the HSV1-sr39tk gene to include the R176Q substitution would exhibit phosphorylation activity predominantly with pyrimidine-based radiotracers. Indeed, cells transduced with such a mutant, HSV1-R176Qsr39tk, showed high ^{3}H-FEAU uptake in vitro, while ^{3}H-PCV accumulation was low. As expected, cells expressing HSV1-R176Qsr39tk mutant showed higher IC_{50} values for GCV and BVdU (∼tenfold) compared to wildtype HSV1-tk-transduced cells. Thus, the retained ability of HSV1-R176Qsr39tk to convert clinically used suicide prodrugs allows eliminating transduced cells when needed.

Then we tested the new HSV1-R176Qsr39tk reporter gene in an animal model. Both PET imaging and tissue sampling measurements demonstrated higher ^{18}F-FEAU uptake compared to its predecessor, HSV1-R176Qtk, and corroborated our in vitro results. We observed a significant decrease in phosphorylating ability of the HSV1-R176Qsr39tk enzyme for acycloguanosine and to a much lesser degree for pyrimidine derivatives compared with the wild-type HSV1-tk (higher selectivity index for HSV1-R176Qsr39tk). Nevertheless, we were able to demonstrate that the HSV1-R176Qsr39tk mutant phosphorylating activity with FEAU is sufficient for successful PET imaging and that ^{18}F-FEAU accumulation is comparable in HSV1-R176Qsr39tk- and wild-type HSV1-tk-expressing tumors. The latter observation allows us to conclude that HSV1-R176Qsr39tk reporter gene imaging with ^{18}F-FEAU will not be affected in future preclinical and clinical applications. In addition, our resultant HSV1-R176Qsr39tk mutant showed minimal residual activity with acycloguanosine derivatives that might influence the ability of using this reporter gene in patients treated with therapeutic doses of GCV. However, we believe that such an approach could be explored further for the development of pyrimidine-specific reporter genes that will allow for successful PET imaging in patients undergoing therapy with acycloguanosine-based analogs.

Encouraged by these findings, we tested the feasibility of PET imaging of two different xenografts composed of cells transduced with HSV1-R176Qsr39tk and the previously

described acycloguanosine-specific HSV1-A167Ysr39tk mutant [25] in the same animals. Noteworthy, our imaging experiments were conducted using xenografts that were formed from cells highly (nearly 100%) transduced with the reporter. We observed high specific uptake of each radiotracer in the corresponding xenograft. Despite the small ^{18}F-FHBG accumulation in HSV1-R176Qsr39tk-expressing tumors, we could easily discriminate the expression of both reporters in the two different transduced xenografts.

There are many areas of application where the pyrimidine-specific reporter can be incorporated into dual PET reporter genetic systems together with acycloguanosine-specific reporter. For example, one could image the localization of transduced antitumor lymphocytes with ^{18}F-FEAU using HSV1-R176Qsr39tk reporter gene as a “beacon” element. Then the tumor-specific activation of lymphocytes at the tumor site could also be monitored using an inducible, pathway-specific promoter driving a HSV1-A167Ysr39tk “sensor” reporter gene with ^{18}F-FHBG. This imaging paradigm could easily be translated into clinical protocols for monitoring the efficacy of adoptive anticancer immunotherapies. Such a dual reporter system can be used as a powerful tool for tracking cells and imaging inducible upregulation of reporter gene expression at the same time.

In conclusion, we have successfully developed and tested a new mutant of HSV1-tk reporter gene, HSV1-R176Qsr39tk. This reporter showed the ability to convert pyrimidine-based nucleoside derivatives, while exhibiting very low phosphorylation activity with acycloguanosine analogs. In combination with acycloguanosine-specific HSV1-A167Ysr39tk reporter, HSV1-R176Qsr39tk mutant can be used for simultaneous PET imaging of two independent cell populations or molecular biological processes in the same living subject using consecutive administration of ^{18}F-FEAU and ^{18}F-FHBG clinical radiotracers.

Acknowledgments

We thank Dr. Ronald Blasberg for his help in manuscript preparation. We thank Dr. Pat Zanzonico for his expert technical assistance and we thank Dr. Juri Gelovani for his long-term support.

Financial support This work was supported by the NIH P50 CA86438-01, R01 CA102352; grants. Technical services provided by the MSKCC Small-Animal Imaging Core Facility, supported in part by NIH Small-Animal Imaging Research Program (SAIRP), grant R24 CA83084 and NIH Center Grant P30 CA08748.

References

1. Edelstein ML, Abedi MR, Wixon J, Edelstein RM. Gene therapy clinical trials worldwide 1989-2004-an overview. J Gene Med. 2004; 6:597–602. [PubMed: 15170730]
2. Tjuvajev JG, Stockhammer G, Desai R, Uehara H, Watanabe K, Gansbacher B, et al. Imaging the expression of transfected genes in vivo. Cancer Res. 1995; 55:6126–32. [PubMed: 8521403]
3. Tjuvajev JG, Avril N, Oku T, Sasajima T, Miyagawa T, Joshi R, et al. Imaging herpes virus thymidine kinase gene transfer and expression by positron emission tomography. Cancer Res. 1998; 58:4333–41. [PubMed: 9766661]
4. Gambhir SS, Barrio JR, Wu L, Iyer M, Namavari M, Satyamurthy N, et al. Imaging of adenoviral-directed herpes simplex virus type 1 thymidine kinase reporter gene expression in mice with radiolabeled ganciclovir. J Nucl Med. 1998; 39:2003–11. [PubMed: 9829598]
5. Gambhir SS, Barrio JR, Herschman HR, Phelps ME. Assays for noninvasive imaging of reporter gene expression. Nucl Med Biol. 1999; 26:481–90. [PubMed: 10473186]

6. Conti PS, Alauddin MM, Fissekis JR, Schmall B, Watanabe KA. Synthesis of 2′-fluoro-5-[11C]-methyl-1-beta-D-arabinofuranosyluracil ([11C]-FMAU): a potential nucleoside analog for in vivo study of cellular proliferation with PET. Nucl Med Biol. 1995; 22:783–9. [PubMed: 8535339]
7. Brust P, Haubner R, Friedrich A, Scheunemann M, Anton M, Koufaki ON, et al. Comparison of [18F]FHPG and [124/125I] FIAU for imaging herpes simplex virus type 1 thymidine kinase gene expression. Eur J Nucl Med. 2001; 28:721–9. [PubMed: 11440032]
8. Mangner TJ, Klecker RW, Anderson L, Shields AF. Synthesis of 2′-deoxy-2′-[18F]fluoro-beta-D-arabinofuranosyl nucleosides, [18F]FAU, [18F]FMAU, [18F]FBAU and [18F]FIAU, as potential PET agents for imaging cellular proliferation. Synthesis of [18F]labelled FAU, FMAU, FBAU, FIAU Nucl Med Biol. 2003; 30:215–24.
9. Choi SR, Zhuang ZP, Chacko AM, Acton PD, Tjuvajev-Gelovani J, Doubrovin M, et al. SPECT imaging of herpes simplex virus type1 thymidine kinase gene expression by [(123)I]FIAU(1). Acad Radiol. 2005; 12:798–805. [PubMed: 16039533]
10. Tjuvajev JG, Doubrovin M, Akhurst T, Cai S, Balatoni J, Alauddin MM, et al. Comparison of radiolabeled nucleoside probes (FIAU, FHBG, and FHPG) for PET imaging of HSV1-tk gene expression. J Nucl Med. 2002; 43:1072–83. [PubMed: 12163634]
11. Min JJ, Iyer M, Gambhir SS. Comparison of [18F]FHBG and [14C]FIAU for imaging of HSV1-tk reporter gene expression: adenoviral infection vs stable transfection. Eur J Nucl Med Mol Imaging. 2003; 30:1547–60. [PubMed: 14579096]
12. Alauddin MM, Shahinian A, Gordon EM, Conti PS. Direct comparison of radiolabeled probes FMAU, FHBG, and FHPG as PET imaging agents for HSV1-tk expression in a human breast cancer model. Mol Imaging. 2004; 3:76–84. [PubMed: 15296672]
13. Gambhir SS, Bauer E, Black ME, Liang Q, Kokoris MS, Barrio JR, et al. A mutant herpes simplex virus type 1 thymidine kinase reporter gene shows improved sensitivity for imaging reporter gene expression with positron emission tomography. Proc Natl Acad Sci USA. 2000; 97:2785–90. [PubMed: 10716999]
14. Haberkorn U, Altmann A, Morr I, Knopf KW, Germann C, Haeckel R, et al. Monitoring gene therapy with herpes simplex virus thymidine kinase in hepatoma cells: uptake of specific substrates. J Nucl Med. 1997; 38:287–94. [PubMed: 9025757]
15. Jacobs A, Voges J, Reszka R, Lercher M, Gossmann A, Kracht L, et al. Positron-emission tomography of vector-mediated gene expression in gene therapy for gliomas. Lancet. 2001; 358:727–9. [PubMed: 11551583]
16. Peñuelas I, Boán J, Marti-Climent JM, Sangro B, Mazzolini G, Prieto J, et al. Positron emission tomography and gene therapy: basic concepts and experimental approaches for in vivo gene expression imaging. Mol Imaging Biol. 2004; 6:225–38. [PubMed: 15262238]
17. Deng WP, Yang WK, Lai WF, Liu RS, Hwang JJ, Yang DM, et al. Non-invasive in vivo imaging with radiolabelled FIAU for monitoring cancer gene therapy using herpes simplex virus type 1 thymidine kinase and ganciclovir. Eur J Nucl Med Mol Imaging. 2004; 31:99–109. [PubMed: 14513292]
18. Koehne G, Doubrovin M, Doubrovina E, Zanzonico P, Gallardo HF, Ivanova A, et al. Serial in vivo imaging of the targeted migration of human HSV-TK-transduced antigen-specific lymphocytes. Nat Biotechnol. 2003; 21:405–13. [PubMed: 12652311]
19. Dobrenkov K, Olszewska M, Likar Y, Shenker L, Gunset G, Cai S, et al. Monitoring the efficacy of adoptively transferred prostate cancer-targeted human T lymphocytes with PET and bioluminescence imaging. J Nucl Med. 2008; 49:1162–70. [PubMed: 18552144]
20. Dubey P, Su H, Adonai N, Du S, Rosato A, Braun J, et al. Quantitative imaging of the T cell antitumor response by positron-emission tomography. Proc Natl Acad Sci USA. 2003; 100:1232–7. [PubMed: 12547911]
21. Doubrovin M, Ponomarev V, Beresten T, Balatoni J, Bornmann W, Finn R, et al. Imaging transcriptional regulation of p53-dependent genes with positron emission tomography in vivo. Proc Natl Acad Sci USA. 2001; 98:9300–5. [PubMed: 11481488]
22. Ponomarev V, Doubrovin M, Lyddane C, Beresten T, Balatoni J, Bornman W, et al. Imaging TCR-dependent NFAT-mediated T-cell activation with positron emission tomography in vivo. Neoplasia. 2001; 3:480–8. [PubMed: 11774030]

23. Green LA, Yap CS, Nguyen K, Barrio JR, Namavari M, Satyamurthy N, et al. Indirect monitoring of endogenous gene expression by positron emission tomography (PET) imaging of reporter gene expression in transgenic mice. Mol Imaging Biol. 2002; 4:71–81. [PubMed: 14538050]
24. Ponomarev V, Doubrovin M, Shavrin A, Serganova I, Beresten T, Ageyeva L, et al. A human-derived reporter gene for noninvasive imaging in humans: mitochondrial thymidine kinase type 2. J Nucl Med. 2007; 48:819–26. [PubMed: 17468435]
25. Likar Y, Dobrenkov K, Olszewska M, Vider E, Shenker L, Cai S, et al. A new acycloguanosine-specific supermutant of herpes simplex virus type 1 thymidine kinase suitable for PET imaging and suicide gene therapy for potential use in patients treated with pyrimidine-based cytotoxic drugs. J Nucl Med. 2008; 49:713–20. [PubMed: 18413388]
26. Kussmann-Gerber S, Kuonen O, Folkers G, Pilger BD, Scapozza L. Drug resistance of herpes simplex virus type 1—structural considerations at the molecular level of the thymidine kinase. Eur J Biochem. 1998; 255:472–81. [PubMed: 9716390]
27. Ponomarev V, Doubrovin M, Serganova I, Beresten T, Vider J, Shavrin A, et al. Cytoplasmically retargeted HSV1-tk/GFP reporter gene mutants for optimization of non-invasive molecular-genetic imaging. Neoplasia. 2003; 5:245–54. [PubMed: 12869307]
28. Riviere, I.; Sadelain, M. Methods for the construction of retroviral vectors and the generation of high titer producers. In: Robbins, PD., editor. Gene therapy protocols: methods in molecular biology. Totowa, NJ: Humana; 1997. p. 59-78.
29. Alauddin MM, Fissekis JD, Conti PS. Synthesis of [18F]-labeled 2′-deoxy-2′-fluoro-5-methyl-1-β-D-arabinofuranosyluracil ([18F]-FMAU). J Label Compd Radiopharm. 2002; 45:583–90.
30. Alauddin MM, Conti PS. Synthesis and preliminary evaluation of 9-(4-[18F]-fluoro-3-hydroxymethylbutyl)guanine ([18F]FHBG): a new potential imaging agent for viral infection and gene therapy using PET. Nucl Med Biol. 1998; 25:175–80. [PubMed: 9620620]
31. Alauddin MM, Shahinian A, Park R, Tohme M, Fissekis JD, Conti PS. In vivo evaluation of 2′-deoxy-2′-[(18)F]fluoro-5-iodo-1-beta-D: -arabinofuranosyluracil ([(18)F]FIAU) and 2′-deoxy-2′-[(18)F]fluoro-5-ethyl-1-beta-D: -arabinofuranosyluracil ([(18)F] FEAU) as markers for suicide gene expression. Eur J Nucl Med Mol Imaging. 2007; 34:822–9. [PubMed: 17206416]
32. Serganova I, Doubrovin M, Vider J, Ponomarev V, Soghomonyan S, Beresten T, et al. Molecular imaging of temporal dynamics and spatial heterogeneity of hypoxia-inducible factor-1 signal transduc-tion activity in tumors in living mice. Cancer Res. 2004; 64:6101–8. [PubMed: 15342393]
33. Balatoni JA, Doubrovin M, Ageyeva L, Pillarsetty N, Finn RD, Gelovani JG, et al. Imaging herpes viral thymidine kinase-1 reporter gene expression with a new 18F-labeled probe: 2′-fluoro-2′-deoxy-5-[18F]fluoroethyl-1-beta-d-arabinofuranosyl uracil. Nucl Med Biol. 2005; 32:811–9. [PubMed: 16253805]
34. Alauddin MM, Shahinian A, Gordon EM, Conti PS. Evaluation of 2′-deoxy-2′-flouro-5-methyl-1-beta-D-arabinofuranosyluracil as a potential gene imaging agent for HSV-tk expression in vivo. Mol Imaging. 2002; 1:74–81. [PubMed: 12920847]
35. Soghomonyan S, Hajitou A, Rangel R, Trepel M, Pasqualini R, Arap W, et al. Molecular PET imaging of HSV1-tk reporter gene expression using [18F]FEAU. Nat Protoc. 2007; 2:416–23. [PubMed: 17406603]
36. Yaghoubi S, Barrio JR, Dahlbom M, Iyer M, Namavari M, Satyamurthy N, et al. Human pharmacokinetic and dosimetry studies of [(18)F]FHBG: a reporter probe for imaging herpes simplex virus type-1 thymidine kinase reporter gene expression. J Nucl Med. 2001; 42:1225–34. [PubMed: 11483684]
37. Yaghoubi SS, Gambhir SS. PET imaging of herpes simplex virus type 1 thymidine kinase (HSV1-tk) or mutant HSV1-sr39tk reporter gene expression in mice and humans using [18F]FHBG. Nat Protoc. 2006; 1:3069–75. [PubMed: 17406570]
38. Alauddin MM, Shahinian A, Kundu RK, Gordon EM, Conti PS. Evaluation of 9-[(3-18F-fluoro-1-hydroxy-2-propoxy)methyl]guanine ([18F]-FHPG) in vitro and in vivo as a probe for PET imaging of gene incorporation and expression in tumors. Nucl Med Biol. 1999; 26:371–6. [PubMed: 10382839]

39. Degreve B, Esnouf R, De Clercq E, Balzarini J. Selective abolishment of pyrimidine nucleoside kinase activity of herpes simplex virus type 1 thymidine kinase by mutation of alanine-167 to tyrosine. Mol Pharmacol. 2000; 58:1326–32. [PubMed: 11093770]

40. Balzarini J, Liekens S, Esnouf R, De Clercq E. The A167Y mutation converts the herpes simplex virus type 1 thymidine kinase into a guanosine analogue kinase. Biochemistry. 2002; 41:6517–24. [PubMed: 12009916]

41. Black ME, Kokoris MS, Sabo P. Herpes simplex virus-1 thymidine kinase mutants created by semi-random sequence mutagenesis improve prodrug-mediated tumor cell killing. Cancer Res. 2001; 61:3022–6. [PubMed: 11306482]

Abbreviations

HSV1-tk	herpes simplex virus type 1 thymidine kinase
GFP	green fluorescent protein
PET	positron emission tomography
FHBG	9-[4-fluoro-3-(hydroxymethyl)butyl]guanine
FEAU	2′-fluoro-2′-deoxy-1-β-D-arabinofuranosyl-5-ethyl-uracil
GCV	ganciclovir
FACS	fluorescence activated cell sorting
MEM	modified Eagle's medium
VSV-G	vesicular stomatitis virus G protein
FCS	fetal calf serum

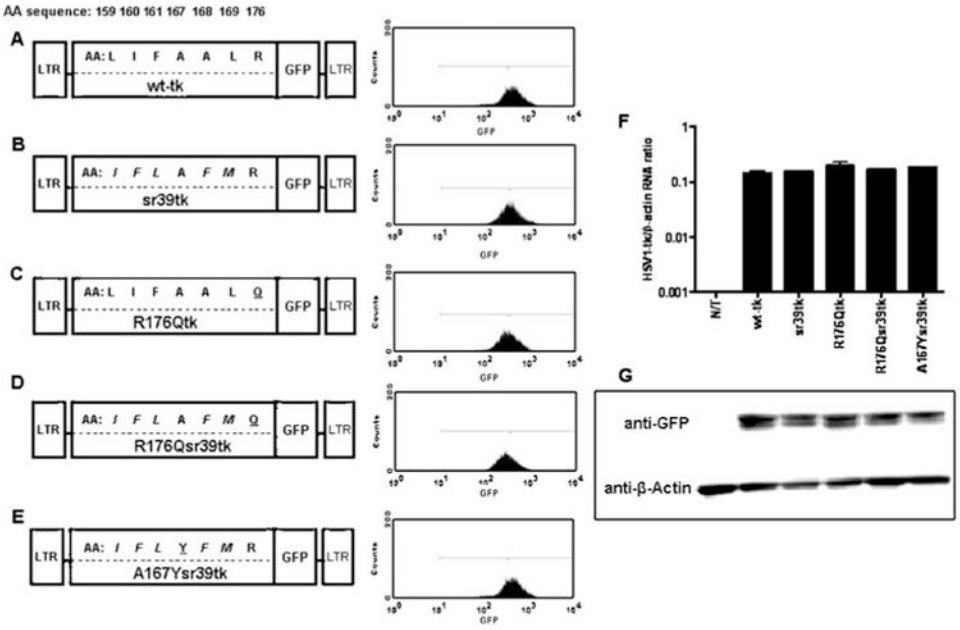

Fig. 1.

Schematic structure of retroviral vectors for mammalian expression, the amino acid differences between wild-type and different HSV1-tkGFP mutants. **a** Wild-type HSV1-tkGFP. **b** HSV1-sr39tkGFP. **c** HSV1-R176QtkGFP. **d** HSV1-R176Qsr39tkGFP. **e** HSV1-A167Ysr39tkGFP reporter genes. Five amino acid substitutions from HSV1-sr39tk are *italicized*; R176Q and A167Y targeted *mutations* are *underlined*. Expression levels were normalized by FACS in transduced U87 cells using a GFP filter set. **f** Quantitative RT-PCR analysis of HSV1-tk mRNA from non-transduced (N/T) and transduced cell populations normalized by β-actin mRNA levels; values expressed as HSV1-tk mRNA/β-actin concentration ratios. **g** Western blot analysis of HSV1-tk/GFP (∼72 kDa) and β-actin (∼42 kDa) proteins expression in non-transduced and transduced cell populations using GFP- and β-actin-specific monoclonal antibodies. *Blot lines correspond to the cell line names* in **f**

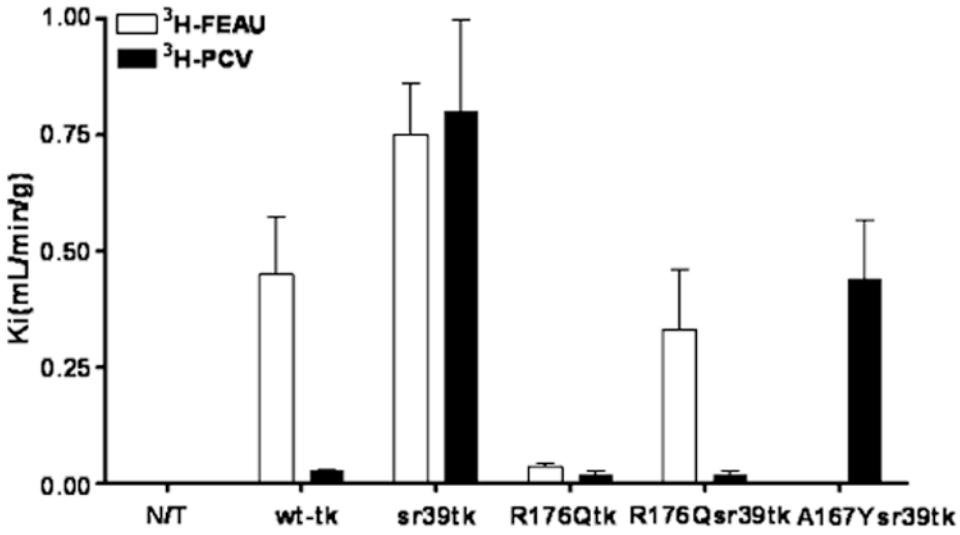

Fig. 2.

Radiotracer uptake (*Ki*) of ^{3}H-FEAU and ^{3}H-PCV in non-transduced (*N/T*) and transduced U87 cells listed on the abscissa. Values are the mean±SD. Representation of at least three independent experiments

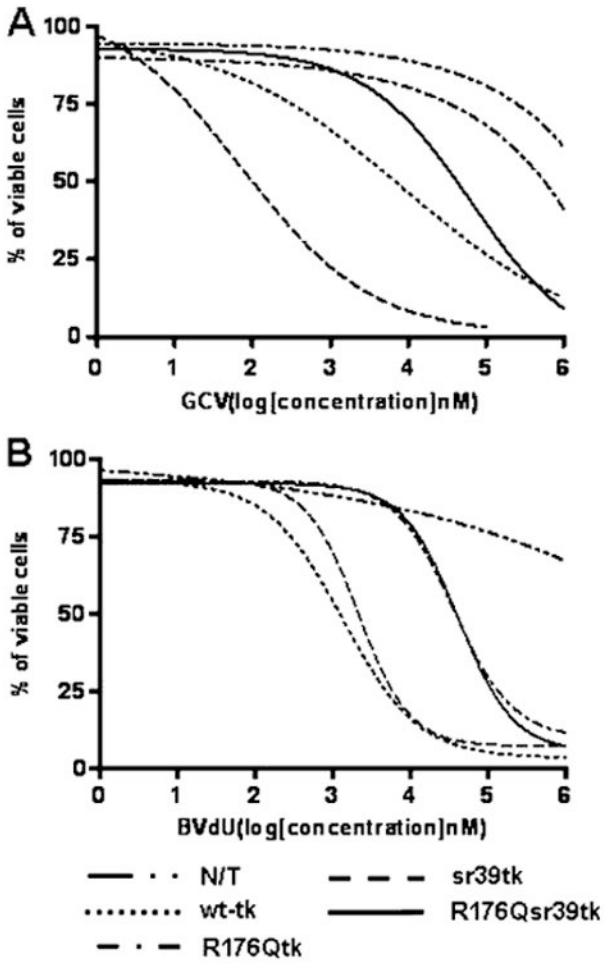

Fig. 3.

Assessment of drug sensitivity of non-transduced (N/T) and transduced U87 cells to GCV (**a**) and BVdU (**b**) nucleoside analogs in vitro. HSV1-sr39tk+ cells showed the lowest IC_{50} for GCV (0.10 μM). IC_{50} values for wild-type HSV1-tk, HSV1-R176Qtk, and HSV1-R176Qsr39tk expressing cells with GCV were 10, 940, and 111 μM, respectively. The IC_{50} for non-transduced cells with GCV was >1 mM. IC_{50} values for wild-type HSV1-tk, HSV1-sr39tk, HSV1-R176Qtk, and HSV1-R176Qsr39tk expressing cells with BVdU were 1.3, 2.1, 91, and 92 μM, respectively. The IC_{50} for non-transduced cells with BVdU was >10 mM. *N/T* non-transduced cells. Representation of three independent experiments

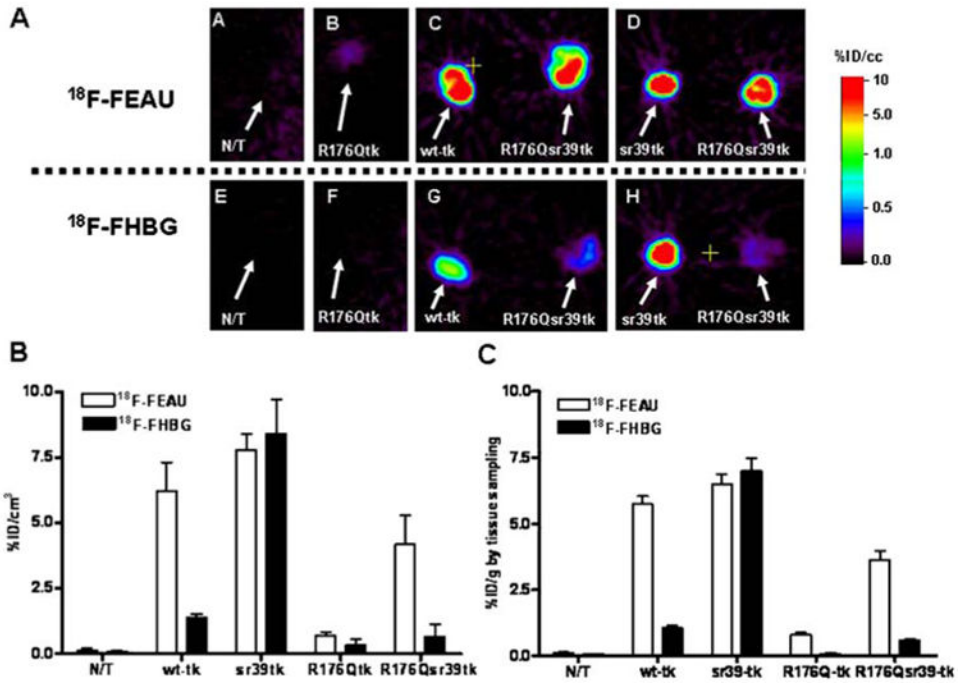

Fig. 4.

MicroPET imaging of reporter gene expression. **A** Axial microPET images through the xenografts placed s.c. over the shoulders are shown: **a**, **e** non-transduced (N/T) and transduced U87 xenografts, including HSV1-R176Qtk (**b**, **f**) and wild-type HSV1-tk (**c**, **g** *left*), HSV1-sr39tk (**d**, **h** *left*), and HSV1-R176Qsr39tk (**c**, **d**, **g**, **h** *right*). ^{18}F-FEAU (*upper row*) and ^{18}F-FHBG (*lower row*) images at 2 h after radiotracer administration are shown for the same animal obtained on consecutive days. All images were adjusted to the same color scale. **B** Image-based measurements of ^{18}F-FEAU and ^{18}F-FHBG at 2 h after radiotracer administration in the same animals expressed as % injected dose/cc of tissue (*%ID/cc*, *n*=5). Values are the mean±SD. **C** Tissue sampling-based measurements of ^{18}F-FEAU and ^{18}F-FHBG accumulation at 2 h after radiotracer administration. Expressed as % injected dose/gram of tissue (*%ID/g*, *n*=5). Values are the mean±SD

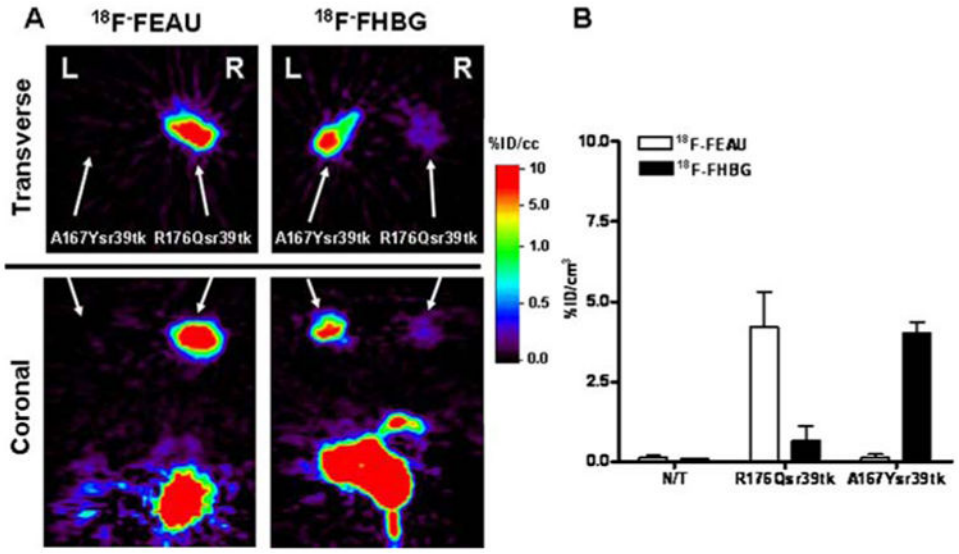

Fig. 5.

MicroPET imaging comparison of HSV1-R176Qsr39tk and HSV1-A167Ysr39tk reporter gene expression in the same animal. a A representative animal bearing a HSV1-R176Qsr39tk- (right shoulder) and a HSV1-A167Ysr39tk- (left shoulder) expressing xenograft was imaged with ^{18}F-FEAU and ^{18}F-FHBG on 2 consecutive days. Axial (transverse) and coronal sections through the tumors are shown. All images were adjusted to the same color scale. High specific ^{18}F-FEAU accumulation was observed in the HSV1-R176Qsr39tk+ xenograft and high specific accumulation of ^{18}F-FHBG was observed in theHSV1-A167Ysr39tk xenograft. Slight ^{18}F-FHBG accumulation was also observed in HSV1-R176Qsr39tk-expressing xenograft. Note radiotracer clearance from gut and bladder. **b** Image-based measurements of ^{18}F-FEAU and ^{18}F-FHBG at 2 h after radiotracer administration expressed as % injected dose/cc of tissue (*%ID/cc*, *n*=5). Values are the mean ±SD. *N/T* non-transduced